Transport of water vapor in the tropical tropopause layer

A. Gettelman, W. J. Randel, F. Wu, and S. T. Massie

National Center for Atmospheric Research, Boulder CO, USA

[1] A trajectory model coupled to a simple micro-physical model is used to explore the observed relationship between convection, water vapor and cirrus clouds in the tropical tropopause layer (TTL). Horizontal transport associated with the local Hadley circulation leads to water vapor minima in the winter hemisphere separated from the convective regions and the region of minimum temperatures. These spatial signatures are consistent with observations of water vapor and cirrus in the TTL from the Halogen Occultation Experiment (HALOE). In the simulations, one third of observed ice is formed due to horizontal transport through cold regions. Applied variations in temperature over time scales longer than a few hours, similar to gravity wave induced perturbations, act to lower the simulated water vapor. *INDEX TERMS:* 3362 Meteorology and Atmospheric Dynamics: Stratosphere/troposphere interactions, 3314 Meteorology and Atmospheric Dynamics: Convective processes, 3374 Meteorology and Atmospheric Dynamics: Tropical meteorology

1. Introduction

[2] It is generally accepted that most air enters the stratosphere in the tropics [*Holton et al.*, 1995] by a combination of rapid vertical motion (on the order of m s^{-1}) in convection and slow diabatic ascent (order 10^{-3} m s^{-1}). The relative roles of these processes are not well understood. Increases in stratospheric water vapor larger than those expected from oxidation of increased methane have been observed over the last 40 years [*SPARC*, 2000]. Yet tropical tropopause temperatures, which are thought to limit the influx of water vapor into the stratosphere by freeze-drying, have been observed to be decreasing [*Randel et al.*, 2000; *Seidel et al.*, 2001]. Given the importance of water vapor for the radiation balance and chemistry of the stratosphere, understanding the cause of these long term trends in water vapor is critical.

[3] Recently, *Holton and Gettelman*, [2001] (hereafter HG) used an idealized two dimensional model to show that horizontal advection could dehydrate air to stratospheric levels. In this work we use a more detailed mechanistic model of ice microphysics applied along three dimensional air parcel trajectories to extend the analysis of HG to climatological relationships between horizontal motion, convection, temperatures, water vapor and cirrus clouds in the tropical tropopause layer (TTL). Our motivation is the observation of minimum water vapor in the TTL northward of active convective regions in January and southward in July [*Randel et al.*, 2001], suggesting the importance of advection by the local Hadley circulation.

[4] Following HG, we define the TTL as the tropical layer between 14–19km. Below the TTL tropospheric processes dominate water vapor, and above the TTL stratospheric processes dominate. Trajectories are calculated using three-dimensional winds from meteorological analyses. The micro-physical model

is constrained by analyzed temperatures along the trajectories. We demonstrate that the model can reproduce the observed climatology of water vapor and ice in the TTL, present diagnostics and sensitivity studies, and discuss the implications for stratospheric water vapor.

2. Model Description

[5] A mechanistic micro-physical model is applied along trajectories to generate maps of water vapor and water ice in the TTL. The model is formulated by parameterizing the large-scale effects of condensation and evaporation processes. It is not a detailed micro-physical model. The model iterates along a trajectory using the following steps: (1) Water vapor in a parcel is compared to the local saturation mixing ratio over ice. If the air is super-saturated by an amount greater than a critical relative humidity (*cRH*) then the excess vapor is transferred to the ice phase with an e-folding time of τ_C. (2) If the air is below 100% RH some ice is evaporated with an e-folding time of τ_E. (3) If any ice remains then some falls out.

[6] Ice fallout is parameterized based on an e-folding time, τ_L, which varies as a function of ice water content (IWC). IWC is a function of the local temperature, pressure and the ice mixing ratio. For IWC $> 3 \times 10^{-4}$ g m^{-3}, large particles are assumed and fallout occurs rapidly (τ_L = 0.33 days). For IWC $< 1 \times 10^{-5}$ g/m^{-3}, small particles are assumed and fallout occurs slowly (τ_L = 10 days). Fallout is ramped linearly for IWC between these limits. Values are chosen to represent observed and modeled fall speeds [*Heymsfield and Iaquinta*, 2000]. This approach captures the observed variation in ice-crystal settling time, and is similar in principle to that used by *Heymsfield and Donner* [1990] for a General Circulation Model.

[7] Three dimensional back trajectories are calculated using winds from the European Center for Medium Range Weather Forecasts (ECMWF). Trajectories are initialized on a 1° by 1° grid from 40°S to 40°N, at pressure levels of 147, 121, 100, 82 and 68 hPa. Back trajectories are run for 10 days. The micro-physical model is applied once per day running forward in time from the end of the back trajectory using the daily minimum analyzed ECMWF temperatures along each trajectory. Additional experiments have also been run using (1) 6-hourly analyses temperatures, and (2) these temperatures interpolated to a 1 hour time step.

[8] The model is initialized along each trajectory by setting the initial water vapor in a parcel to 50% relative humidity in the troposphere and TTL (below 10km poleward of 20° latitude, and below 20km equator-ward of 20° latitude). The initial mixing ratio of parcels in the stratosphere is 4 ppmv. These values are similar to observations [*SPARC*, 2000].

[9] A stochastic perturbation, normally distributed with a standard deviation of 2°C (σ_t = 2), is applied to the temperature to represent variations due to hypothetical gravity waves which occur on time and space scales smaller than the global analysis fields used as input. The ECMWF analyses do not resolve variability on timescales shorter than 12 hours (the frequency of radiosonde data) and space scales smaller than several hundred kilometers. The value of σ_t is similar to temporal variability observed from high

frequency (6 hourly) radiosondes [*Tsuda et al.*, 1994] or kilometer scale spatial variability observed from aircraft [*Pfister et al.*, 2001].

[10] The e-folding time for evaporation of ice is one day ($\tau_E = 1$) and the critical relative humidity for ice formation is set at 110% ($cRH = 110\%$). The condensation e-folding time is 0.3 days ($\tau_C = 0.3$). These values are chosen to represent realistic timescales similar to previous observations and model studies [*Jensen et al.*, 1994]. The 1° by 1° results are averaged over 4° by 10° boxes for comparison to observations. Monthly results are the average of runs initialized on the 10th, 20th and 30th of each month. As input we use analyses from January 1989, 1990, 1992, 1998, 1999 and July 1998, 1999, representing a mix of warm and cold phases of the El-Niño Southern Oscillation (ENSO).

3. Results

[11] The distribution of water vapor in the TTL observed from the Halogen Occultation Experiment (HALOE) is illustrated in Figure 1. The reliability of horizontal gradients observed by HALOE at these altitudes is good [*Randel et al.*, 2001], with data retrieved nearly 90% of the time at 100 hPa. January 100 hPa observations of water vapor in the TTL from HALOE version 19 data averaged over 1992–1999 (Figure 1a) show a distinct minimum in the Western Pacific, centered near 10°N (also noted by *Jackson et al.* [1998] and *Randel et al.* [2001]). The minimum is
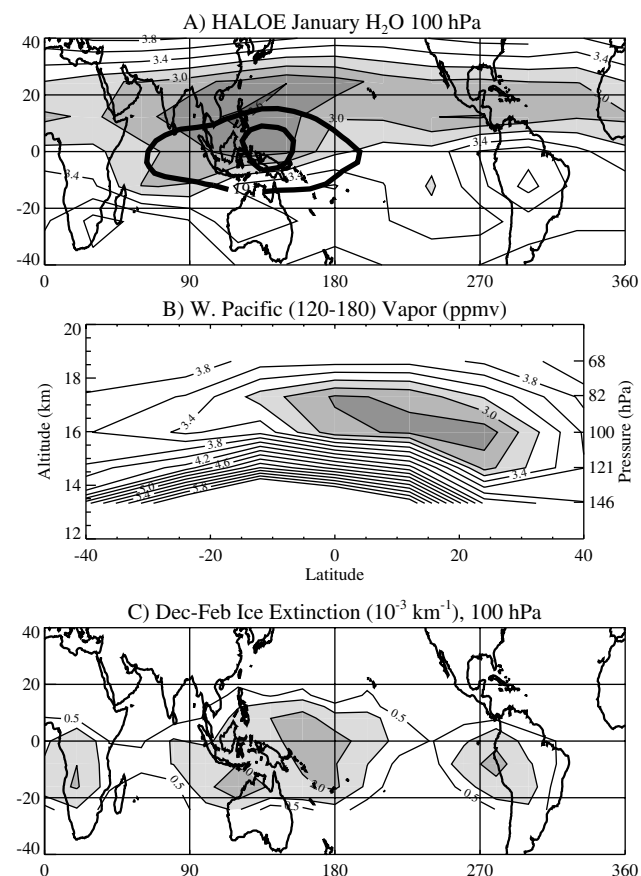

Figure 1.   (a) January mean water vapor from HALOE at 100hPa (ppmv). Water vapor below 3.4 ppmv is shaded. Contours are at intervals of 0.2 ppmv. Thick lines are 190°K and 191°K temperature contours from ECMWF analyses. (b) Regional mean January water vapor (ppmv) for the Western Pacific (120–180°E), contour interval and shading as in (a). (c) Seasonal (December–February) HALOE aerosol extinction coefficient due to cirrus clouds at 100hPa. Contours at 0.5, 1 and 2 × 10^{-3} km^{-1}, shaded above 1 × 10^{-3} km^{-1}.
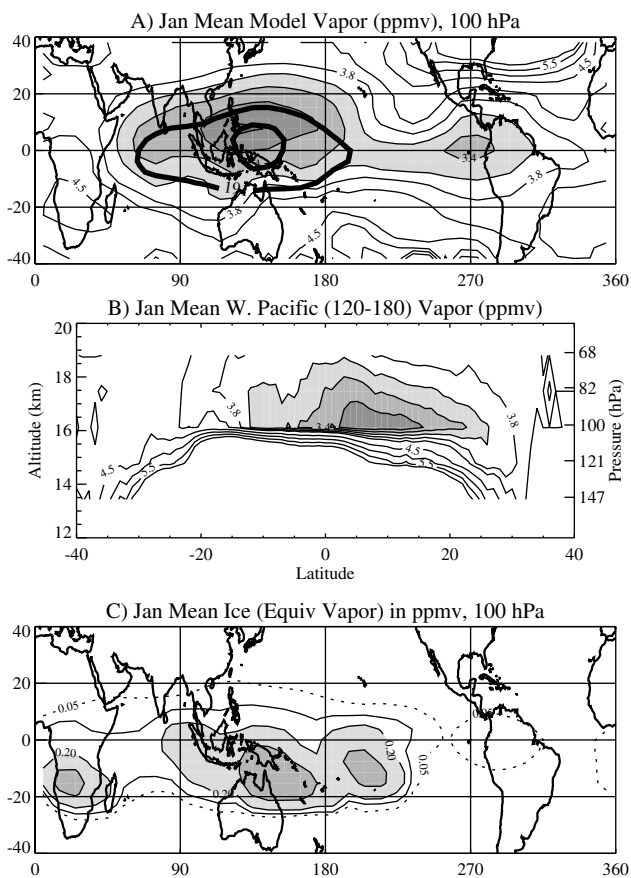

Figure 2.   (a) January simulated water vapor at 100hPa (ppmv). Water vapor below 3.8 ppmv is shaded. Contours are at intervals of 0.2 ppmv up to 4ppmv, then every 0.5 ppmv. Thick lines are 190°K and 191°K temperature contours. (b) Regional water vapor (ppmv) for the Western Pacific (120–180°E), contour interval as in (a). (c) Cirrus ice (equivalent water vapor) at 100hPa. Contours at 0.05 (dotted), 0.1, 0.2 and 0.5 ppmv, shaded above 0.2 ppmv.

found at lower altitudes away from the equator (Figure 1b), consistent with motion along isentropic trajectories which slope downward and poleward. However, the coldest temperatures at 100 hPa are nearly symmetric around the equator in the Western Pacific (Figure 1a). Most convection in January is observed south of the equator. HALOE aerosol extinction measurements (Figure 1c) suggest that cirrus clouds lie above and adjacent to the convective regions (see *Massie et al.* [2000]), although thin cirrus clouds need not be directly connected to convection [*Winker and Trepte*, 1998].

[12] The water vapor distribution in the TTL simulated over 5 Januaries is illustrated in Figure 2. Water vapor is lowest in the simulations at 100hPa, which is the level closest to the observed cold point. The minimum in water vapor is shifted north of the equator in the Western Pacific, similar to observations (Figure 1a). The minimum is centered over the northern edge of the coldest region, downstream for the northward Hadley circulation and therefore consistent with results from HG. There is a secondary minimum over the equator near South America, which is also present in the observations, though the observed minimum (Figure 1a) is north of the equator. A vertical cross section in the Western Pacific (Figure 2b) indicates that the minimum simulated water vapor in the Western Pacific extends poleward and downward in the northern hemisphere, consistent with observations (Figure 1b).

[13] Figure 2c illustrates cirrus ice as equivalent water vapor (ppmv). This quantity is different than the cirrus extinction measurements shown in Figure 1c, but the spatial patterns are similar (maxima over convection). Simulated cirrus ice (Figure 2c)

is formed along a trajectory when parcels rise rapidly from lower levels in the troposphere to higher levels in the TTL. Cirrus is also formed from in-situ production of ice by horizontal motion through a cold region. The water found in the cirrus is about 5–15% of the water in the vapor phase at 100 hPa. In Figure 2c, 36% of the ice mass is in parcels whose vertical motion is less than 2km in the last 5 days, i.e. they have not experienced rapid vertical motion (convection) during this time. Cirrus with greater than 0.2 ppmv equivalent water vapor in the model is a result of rapid vertical motion, and confined to regions of significant southern hemisphere convection over the Western Pacific and Africa. Over 1 day, 5–10% of the cirrus ice evaporates.

[14] The model is also able to simulate the water vapor distribution in the TTL during July, the warm period in the annual cycle. In July (Figure 3a), maxima in water vapor in the TTL are observed by HALOE in the northern hemisphere associated with the Indian and North American monsoon circulations. The July minimum in water vapor in the TTL is found over Indonesia just south of the equator. The simulation (Figure 3b) is broadly able to reproduce these relationships. Simulated water vapor in July is higher than observations in the subtropics due to intrusions of wetter air from high latitudes, especially in the southern hemisphere (Figure 3b). Cirrus ice distributions (not shown) in July are concentrated over India and South East Asia in both observations and the simulation.

4. Sensitivity

[15] Detailed sensitivity analyses have been conducted on the various model parameters. As long as the length of the trajectory is as long as the fallout time scale for small IWC (8–10 days), the results are not sensitive to the length of the trajectory. With global analyses as input, the model is not critically sensitive to the particular time step chosen. Time steps of 1 hour, 6 hours and 24 hours have been tested. Using analysis temperatures every 6 hours rather than the minimum daily temperature, raises the simulated water vapor concentrations (RMS difference of 0.6 ppmv) but does not qualitatively change the distribution or any of the conclusions. Small time scale variance does not increase with smaller timesteps, except as proscribed using σ_t (discussed below), because the
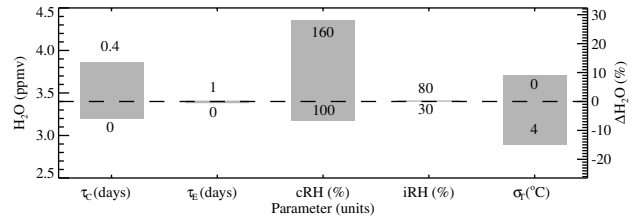
Figure 4. Mean January 100hPa water vapor in the Western Pacific (120–180°E, 20°S–20°N) for various model runs. Extremes of each parameter indicated by values on plot. Dashed line indicates base run value (Figure 2) of 3.4 ppmv.

analysis temperatures have no variance below 6 hours. The water vapor field is not critically sensitive to the parameterization of ice fallout (this mostly affects the quantitative values of the retained ice field).

[16] Sensitivity to the major model parameters is indicated by changes to the average water vapor concentration over the tropical Western Pacific (120–180°E, 20°S–20°N) in Figure 4. This metric yields results similar to an RMS difference from the base case of the model. In all cases, the qualitative distribution is similar to Figure 2. The model is not sensitive to the evaporation time (τ_E) or the initial TTL relative humidity (iRH). The cRH (varied from 100–160%) affects the quantity of water vapor in the TTL, but not the location of the minimum or the horizontal gradients. The condensation time (τ_C) also affects the average water vapor in the Western Pacific (Figure fig:box). For $\tau_C > 0.2$ days, rapid vertical motion is faster than condensation, and greater supersaturations occur. This moistens the region of vertical motion (over convection) south of the equator. The minimum in the northern hemisphere is unchanged for all values of τ_C, but the changes south of the equator raise the average water vapor value in the Western Pacific as τ_C is increased.

[17] Figure 4 also indicates that stochastic variations of the temperature field in the base case (σ_t) reduce the minimum water vapor amount by 0.4 ppmv (~10%) relative to a case with no temperature variance. Consistent with previous studies of cirrus cloud temperature perturbations [Jensen et al., 1996], this occurs only for perturbations lasting 6 or 24 hours, and not for perturbations at 1 hour.

5. Discussion

[18] The simple model reproduces many of the major features of the observed water vapor distribution in the TTL. The simulated water vapor minima in January are shifted into the northern hemisphere as observed. This is due to (1) transport of dry air northward by the local Hadley circulation; (2) dehydration of air by horizontal motion through cold regions north of the equator; and (3) moistening of air over convection in the Southern Hemisphere by rapid vertical transport. The minimum extends poleward and downward, approximately following sloping isentropes originating near the tropical tropopause. The simulation is also able to broadly reproduce the equatorial minimum in water vapor in July, with maxima in the northern hemisphere. One-third of the ice in the simulation (the precursor to dehydration) forms by horizontal advection of air though cold regions, in agreement with the mechanism proposed by HG. However, since not all air in the TTL passes through this cold region, the mechanism proposed by HG is only part of the overall dehydration process. Rapid vertical motion removes much of the water vapor at levels below 100 hPa, but at 100 hPa the supply of water vapor and evaporating ice moistens the TTL in the region of rapid vertical motion south of the equator. Trajectories do not imply much rapid uplift over equatorial South America, so simulated cirrus and water vapor are lower than observations.

A) HALOE July H₂O 100 hPa

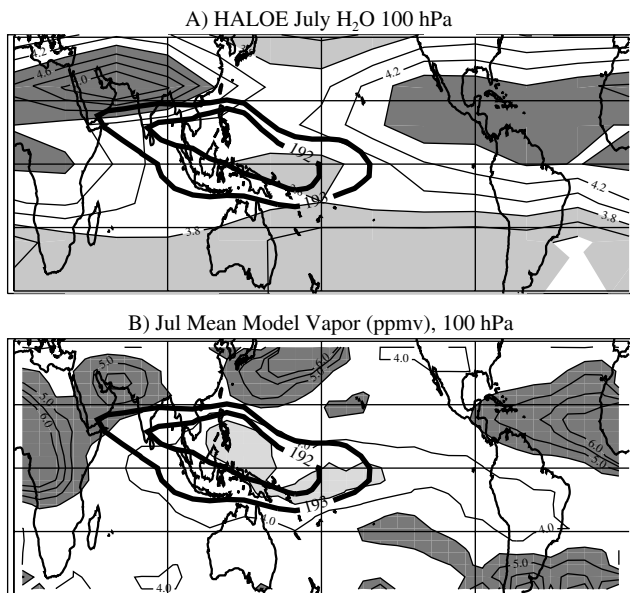B) Jul Mean Model Vapor (ppmv), 100 hPa

Figure 3. July water vapor at 100hPa for (a) HALOE observations and (b) Mechanistic Model. Light shading below 3.8 ppmv, dark shading above 4.4 ppmv. Thick lines are the 192 and 193°K temperature contours.

[19] Quantitatively, water vapor values are sensitive to temperatures and temperature variance. Higher variability of temperatures (i.e., the presence of transient temperature minima) on timescales longer than several hours tends to dry the TTL, indicating that temperature fluctuations from gravity waves in the TTL not captured in global analyses may be important for dehydration. In January, the simulation is about 0.5ppmv wetter at 100hPa than observations, which is consistent with 100 hPa trajectory minimum temperatures that are ~1°C warmer than cold point temperatures from radiosondes [*Seidel et al.*, 2001]. A run using 6 hourly analysis temperatures is about 0.6 ppmv wetter than the base run using daily minimum temperatures, consistent with warmer average temperatures. In July, minimum simulated temperatures and water vapor are similar to observations.

[20] Changes to several of these processes might be causing observed increases in water vapor in the stratosphere independent of tropopause temperatures. A decrease in the temperature variance would result in an increase in water vapor in the TTL and the stratosphere above. However, variations in transport and convection may determine the final water vapor in a parcel. Convection in the summer hemisphere moistens the TTL significantly throughout its depth. If this moistening effect increases due to changes in convective frequency or its altitude, then the water vapor concentration entering the stratosphere may increase even if tropopause temperatures are cooling.

References

Heymsfield, A. J., and L. J. Donner, A scheme for parameterizing ice-cloud water content in general circulation models, *J. Atmos. Sci.*, *47*, 1865–1877, 1990.

Heymsfield, A. J., and J. Iaquinta, Cirrus crystal terminal velocities, *J. Atmos. Sci.*, *57*, 916–938, 2000.

Holton, J. R., and A. Gettelman, Horizontal transport and dehydration in the stratosphere, *Geophys. Res. Lett.*, *28*, 2799–2802, 2001.

Holton, J. R., P. H. Haynes, A. R. Douglass, R. B. Rood, and L. Pfister, Stratosphere-troposphere exchange, *Rev. Geophys.*, *33*, 403–439, 1995.

Jackson, D. R., S. J. Driscoll, E. J. Highwood, J. E. Harries, and J. M. Russell III, Troposphere to stratosphere transport at low latitudes as studied using HALOE observations of water vapour 1992–1997, *Q. J. R. Meteorol. Soc.*, *124*, 169–192, 1998.

Jensen, E. J., O. B. Toon, D. L. Westphal, S. Kinne, and A. J. Heymsfield, Microphysical modeling of cirrus 1. comparison with 1986 FIRE IFO measurements, *J. Geophys. Res.*, *99*, 10,421–10,442, 1994.

Jensen, E. J., O. B. Toon, L. Pfister, and H. B. Selkirk, Dehydration of the upper troposphere and lower stratosphere by subvisible cirrus clouds near the tropical tropopause, *Geophys. Res. Lett.*, *23*, 825–828, 1996.

Massie, S., P. Lowe, X. X. Tie, M. Hervig, G. Thomas, and J. M. Russell III, The effect of the 1997 El Niño on the distribution of upper tropospheric cirrus, *J. Geophys. Res.*, *105*, 22,725–22,741, 2000.

Pfister, L., et al. Aircraft observations of thin cirrus clouds near the tropical tropopause, *J. Geophys. Res.*, *106*, 9765–9786, 2001.

Randel, W. J., F. Wu, and D. J. Gaffen, Interannual variability of the tropical tropopause derived from radiosonde data and NCEP reanalyses, *J. Geophys. Res.*, *105*, 15,509–15,523, 2000.

Randel, W. J., A. Gettelman, F. Wu, J. M. Russell III, J. Zawodny, and S. Oltmans, Seasonal variation of water vapor in the lower stratosphere observed in Halogen Occultation Experiment data, *J. Geophys. Res.*, *106*, 14,313–14,325, 2001.

Seidel, D. J., R. J. Ross, J. K. Angell, and G. C. Reid, Climatological characteristics of the tropical tropopause as revealed by radiosondes, *J. Geophys. Res.*, *106*, 7857–7878, 2001.

SPARC, *Assessment of Water Vapor in the Upper Troposphere and Lower Stratosphere*, WMO/TD-1043, Stratospheric Processes and Their Role In Climate, World Meteorological Organization, Paris, 2000.

Tsuda, T., Y. Murayama, H. Wiryosumarto, S. W. B. Harijono, and S. Kato, Radiosonde observations of equatorial atmosphere dynamics over indonesia: 2. characteristics of gravity waves, *J. Geophys. Res.*, *99*, 10,507–10,516, 1994.

Winker, D. M., and C. R. Trepte, Laminar cirrus observed near the tropical tropopause by LITE, *Geophys. Res. Lett.*, *25*, 3351–3354, 1998.

————————

A. Gettelman, W. J. Randel, F. Wu, and S. T. Massie National Center for Atmospheric Research, Box 3000, Boulder, CO, 80307-3000. (andrew@ ucar.edu)